



More frequent flash flood events and extreme precipitation favouring atmospheric conditions in temperate regions of Europe

Judith Meyer^{1,2}, Malte Neuper³, Luca Mathias⁴, Erwin Zehe³, Laurent Pfister^{1,2}

¹ Catchment and Ecohydrology Group (CAT), Environmental Research and Innovation, Luxembourg Institute of Science and Technology (LIST), Belvaux, 4422, Luxembourg

² Faculty of Science, Technology and Medicine (FSTM), University of Luxembourg, Esch-sur-Alzette, 4365, Luxembourg

³ Institute of Water Resources and River Basin Management, Karlsruhe Institute of Technology (KIT), Karlsruhe, Germany

⁴ Air Navigation Administration, MeteoLux, Findel, Luxembourg

10 *Correspondence to:* Judith Meyer (judith.meyer@list.lu)

Abstract: In recent years, flash floods repeatedly occurred in temperate regions of central western Europe. Unlike in Mediterranean catchments, this flooding behaviour is unusual. In the past, and especially in the 1990s, floods were characterized by predictable, slowly rising water levels during winter and driven by westerly atmospheric fluxes (Pfister et al., 2004). The intention of this study is to link the recent occurrence of flash floods in central western Europe to extreme precipitation and specific atmospheric conditions to identify the cause for this apparent shift. Therefore, we hypothesise that a change in atmospheric conditions led to more frequent extreme precipitation events that subsequently led to more flash flood events in central western Europe. To test this hypothesis, we compiled data on flash floods in central western Europe and selected precipitation events above 40 mm h^{-1} from radar data (RADOLAN, DWD). Moreover, we identified proxy parameters representative for flash flood favouring atmospheric conditions from the ERA5 reanalysis dataset. High specific humidity in the lower troposphere ($q \geq 0.004 \text{ kg kg}^{-1}$), sufficient latent instability ($\text{CAPE} \geq 100 \text{ J kg}^{-1}$) and weak deep-layer wind shear ($\text{DLS} \leq 10 \text{ m s}^{-1}$) proved to be characteristic for long-lasting intense rainfall that can potentially trigger flash floods. These atmospheric parameters, as well as the flash flood and precipitation events were then analysed using linear models. Thereby we found significant increases in atmospheric moisture contents and increases in atmospheric instability. Parameters representing the motion and organisation of convective systems remained largely unchanged in the time period from 1981-2020. Moreover, a trend in the more frequent occurrence of flash floods was confirmed. The number of precipitation events, their maximum 5-minute intensities as well as their hourly sums were however characterized by large inter-annual variations and no trends could be identified between 2002-2020. This study therefore shows that the link from atmospheric conditions leading to extreme precipitation and subsequent flash floods cannot be traced down in an isolated way. The complexity of interactions is likely higher and future analyses should include other potentially relevant factors such as intra-annual precipitation patterns or catchment specific parameters.



1 Introduction

Flash floods rank among the most destructive hazards originating from deep moist convection, leading to economic losses, damage to infrastructure, and high mortality rates (Gaume et al., 2009; Hall, 1981; Llasat et al., 2014; WMO, 2017). They are often accompanied by massive erosion and other geomorphologic processes, such as landslides (Bucala-Hrabia et al., 2020; 35 Vogel et al., 2017). While flash floods remain rather exceptional, their occurrence has more than doubled in Europe since the beginning of the 21st century in comparison to the late 1980s (Marchi et al., 2010; Owen et al., 2018). In Europe, flash floods have to be categorized according to local climate characteristics: Mediterranean Flash Floods (typically occurring in the Mediterranean – including Catalonia, Crete, Southern France, Italy, Slovenia) and Continental Flash Floods (limited to the inland, or continental regions –including Austria, Romania, and Slovakia) (Marchi et al., 2010).

40 Flash flood events in the Mediterranean region, such as the Cévennes, Gard or Aude floods (Alfieri et al., 2011; Nuissier et al., 2008; Séchet, 2019), are usually characterised by warm and very moist air masses being advected from the Mediterranean Sea (Van Delden, 2001; Ducrocq et al., 2008; Marchi et al., 2010; Nuissier et al., 2008). When these air masses encounter orographic lift by geographic barriers such as the Pyrenees, the Massif Central or the Alps, they can cause exceptional amounts of precipitation – potentially covering several 100 km² (Marchi et al., 2010). Within hours, these precipitation events can 45 account for more than 20 % of the annual local precipitation and considerably affect the annual water balance (Marchi et al., 2010). Additionally, when soils are dried-out following dry spells at the end of the summer, infiltration capacities are low and rapidly lead to surface runoff and subsequent flash floods (Borga et al., 2007; Marchi et al., 2010).

In comparison to Mediterranean events, severe convective storms leading to continental flash floods typically affect much smaller areas (a few to 100 km²) and generally last less than seven hours (Marchi et al., 2010). Caused by conditionally unstable 50 atmospheric conditions mainly between May and July, they do not substantially affect the annual water balance. High pre-event soil moisture – caused by rainy weather in the preceding days – may lead to a rapid saturation of soils and a swift onset of extreme runoff response (Marchi et al., 2010). Examples of continental flash floods in recent years relate to Luxembourg around June 2018 (Pfister et al., 2020) and July 2016 (Pfister et al., 2018), to Braunsbach (Germany) in May 2016 (Bronstert et al., 2017, 2018) or the Starzel river flood in June 2008 (Ruiz-Villanueva et al., 2012).

55 While in western Europe large scale winter inundations were the most common flood type until the 1990s (Pfister et al., 2004), (continental) flash flood events have increasingly occurred over the last 15 years (Göppert, 2018; Marchi et al., 2010). This raises the question about the origin of this change in flooding type (Bertola et al., 2020, 2021). In this study, we conjecture that changes in the average atmospheric conditions may lead to flash flood prone meteorological conditions more frequently. Precipitation events potentially causing flash floods are characterized by high rainfall amounts in a short period of time. This 60 is accomplished by high rainfall intensities, which also last over a longer period of time (Doswell et al., 1996; Markowski and Richardson, 2010). That is mostly the case during rainfall events of convective origin. In particular, slow-moving or quasi-stationary multicellular storms can combine both, high rainfall intensities and a sufficiently long duration. Therein, combined effects of several physical processes can cause the most severe rainfall, eventually initiating flash floods. One of these effects



consists of storm training, i.e. propagation may cancel out the advection of the new convective cells, which then consecutively
65 move over the same area. This effect is especially pronounced in the case of rear propagation or back building with the forward
movement being neglected by a backward development of a new cell, leading in the end to slow ground relative speeds of the
whole region of precipitation. Another effect consists of the merging of two or more convective cells. Varying raindrop sizes
and dynamics of merging cells can cause downdrafts producing extremely high precipitation intensities (Doswell et al., 1996;
Markowski and Richardson, 2010). This was the case during the flash flood events in Luxembourg in 2016 and 2018 (Mathias,
70 2019, 2021).

Atmospheric conditions associated with excessive convective rainfall have three major characteristics: (1) latent instability,
(2) high moisture content and (3) a slow storm motion (Van Delden, 2001; Doswell et al., 1996; Markowski and Richardson,
2010; Taszarek et al., 2021a). For deep moist convection to occur, first, the tropospheric lapse rates need to be sufficiently
steep and a lifting mechanism is required (Van Delden, 2001). Second, the moisture content in the boundary layer needs to be
75 abundant in order to supply water vapour for condensation during the lifting process. High to moderate values of relative
humidity in the mid troposphere can further nurture convective cells through limiting water vapour losses due to evaporation
and entraining dry air around convective cell boundaries (Doswell et al., 1996; Markowski and Richardson, 2010; Púčik et al.,
2015). The same effect – limiting the diminishment of specific humidity by entrainment – is realized by a wide updraft.
Additionally, high freezing levels and low cloud base heights enhance the warm cloud depth and thus allowing the warm rain
80 process of collision and coalescence to be more dominant. This leads to a higher precipitation efficiency and is associated with
higher rainfall rates (Doswell et al., 1996; Markowski and Richardson, 2010). In continental Europe, high values of total
column water vapour are often related to the advection of warm Mediterranean air masses (Van Delden, 2001) or air masses
from the subtropical region of the North Atlantic (Mathias, 2021; Mohr et al., 2020). Lastly, to ensure a sufficient duration of
the rainfall event, a slow storm motion is needed (Van Delden, 2001). This generally occurs in case of very weak
85 pressure/geopotential gradients when the mean wind speed and the bulk shear between the surface and the lower to mid
troposphere are weak. Moreover, a decoupled flow (rapid vertical shift of prevailing wind directions by at least 90 degrees)
between the lower and mid troposphere can significantly reduce storm motion in some cases, as analysed by Mathias (2019).
Proxy parameters from climate reanalysis data are regularly used to identify the atmospheric conditions described above during
convective events (Brooks, 2009; Groenemeijer and van Delden, 2007; Púčik et al., 2015; Taszarek et al., 2017; Westermayer
90 et al., 2017). The main parameters used in these studies are the bulk wind shear to estimate the thunderstorm cell organisation
and precipitation efficiency, and convective available potential energy (CAPE), to identify atmospheric instability. Púčik et al.
(2015) found heavy precipitation to occur across a wide range of deep-layer wind shear (DLS; bulk shear between the surface
and 6 km height). This was confirmed by Westermayer et al. (2017) who specifically identified high and low values of DLS
to favour deep moist convection. Low-level wind shear (LLS; bulk shear between the surface and 1 km height) shows similar
95 patterns (Westermayer et al., 2017), but is not indicating the severity of a rainfall event (Púčik et al., 2015). CAPE, as a proxy
for latent instability, needs to be reasonably high for thunderstorms to develop (Púčik et al., 2015; Westermayer et al., 2017),
with values varying between 200-400 J kg⁻¹ already being sufficient (Westermayer et al., 2017). In conditions with higher



CAPE, thunderstorms are more likely to develop (Púčik et al., 2015). Westermayer et al. (2017) identified environments of
CAPE $> 400 \text{ J kg}^{-1}$ and convective inhibition (CIN) $> -50 \text{ J kg}^{-1}$ to be the most supportive for thunderstorms. Since abundant
100 CIN can prevent the formation of thunderstorms even in presence of sufficient CAPE, it must be considered in this study.
When focussing on heavy precipitation events within the range of thunderstorms, specific or relative humidity are parameters
to identify moisture content at different atmospheric levels. Púčik et al. (2015) identified high absolute humidity levels in the
boundary layer and high relative humidity values at low and mid tropospheric levels to be characteristic during heavy
precipitation events. Moreover, Westermayer et al. (2017) found that dry mid-level air (relative humidity $< 50 \%$) can suppress
105 formation of convective storms. So far, studies only included the wind speed in the form of wind shear as a proxy parameter
for the potential organisation of convective systems, which is important for hail, severe gusts and tornadoes. However, the
development of flash floods relies on long-lasting, extreme precipitation. Therefore, the storm motion must be slow, which is
dependent on a weak flow in the lower to mid troposphere. Hence, we consider the wind speed as a relevant parameter when
assessing the flash flood hazard via a slow storm motion.

110 Using the identified atmospheric parameters, it is possible to analyse parameters over a longer period and look for trends or
oscillations. Therein, especially trends in atmospheric instability are debated. While several studies find increasing CAPE in
reanalysis data, recent studies by Taszarek et al. (2021) and Chen et al. (2020) point out, that CAPE is opposed by increasing
CIN. This is observed even to the point where CIN likely suppresses the formation of thunderstorms in seemingly more unstable
conditions in terms of higher CAPE (Taszarek et al., 2021a) and may even lead to an effective reduction in the overall number
115 of thunderstorms and light thunderstorms (Chen et al., 2020; Taszarek et al., 2021a). However, strongly increased CAPE
triggers more intense thunderstorms despite high CIN levels (Chen et al., 2020). In addition, relative humidity levels decrease
at low levels of the atmosphere, connected to rising temperatures, which also reduces the number of thunderstorms (Taszarek
et al., 2021a). In contrast and without considering the effects of CIN, Rädler et al. (2018) found, that the increase in instability
(CAPE) is high enough to not be suppressed by decreases in relative humidity. Changes in wind shear were found to be minor
120 (Rädler et al., 2018). Rädler et al. (2018) concluded, that the frequency of thunderstorms did not increase significantly over
the past 40 years in central western Europe, but that they are more likely to produce severe weather.

So far, most studies have focussed on thunderstorm conditions in general or convective hazards related to lightning, hail,
tornadoes, or wind gusts. Here, we focus on the thunderstorm events that cause extreme precipitation and especially flash flood
events. Forecasting potential heavy precipitation based on atmospheric conditions remains a major challenge, as different
125 atmospheric constellations (e.g. back-building multicells, chaotic cell clustering, atmospheric rivers) can cause heavy
precipitation events, while large hail, for example, is mostly associated with supercells, and therefore less challenging to
identify (Púčik et al., 2015).

In view of these recent findings, we hypothesise that a change in atmospheric conditions led to more frequent extreme
precipitation events that subsequently led to more flash flood events in central western Europe.. Prior to hypothesis testing, we
130 have compiled a comprehensive set of 40 years-worth hydro-climatological observation series – including extreme
precipitation events, related atmospheric conditions and documented flash flood occurrences. We then leveraged this dataset

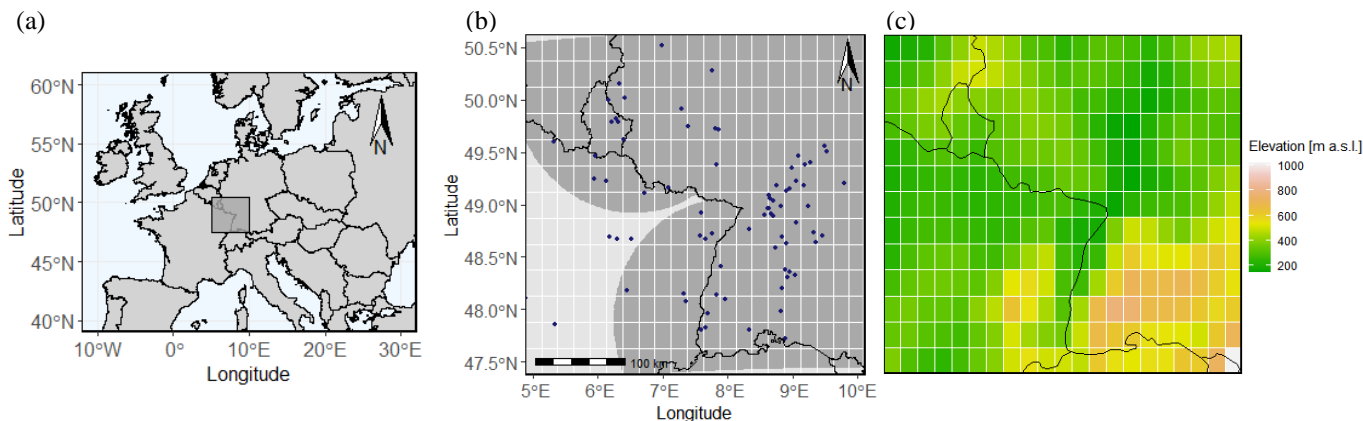


for investigating a potential increase in extreme precipitation events and flash floods in central western Europe. Secondly, we relied on proxy parameters, such as the K-Index, specific humidity, and wind speed, for identifying the atmospheric conditions that had prevailed during extreme precipitation and related flash flood events. Third, we applied a trend analysis to the identified set of atmospheric parameters using the ERA5 reanalysis data (Hersbach et al., 2020) for the past (1981-2020). The overarching goal of our study is to contribute to a better apprehension of climate change effects, as expressed through modifications in the frequency and severity of extreme precipitation and flash flood events in a temperate climate – more specifically in an area where flash floods used to be an extremely rare phenomenon until recently.

2 Data and Methods

140 2.1 Study area and period

Our study area comprises central western Europe (50.5° N, 10° E, 47.5° S, 5° W) including Luxembourg, south-western Germany, and north-eastern France (Figure 1 a-c). The study period spans the summer months from May to August, that exhibit the most favourable conditions for thunderstorms and the onset of flash floods (Van Delden, 2001; Rauber et al., 2008), between 1981 and 2020.



145 **Figure 1:** (a) Location of the study area (dark grey square) within Europe. (b) Map of the study area including data points of occurred flash floods and the range of the DWD-RADOLAN precipitation radar data in dark grey. The white grids show the grid width of the ERA5 reanalysis dataset. (c) Model-topography within the study area based on the ERA5 geopotential.

2.2 Database

150 We downloaded the ERA5 *atmospheric reanalysis data* from the Copernicus' Climate Data Store (CDS) on single levels (Hersbach et al., 2018b) and on different pressure levels (Hersbach et al., 2018a). In addition, we downloaded land data from ERA5 (Muñoz Sabater, 2019) to analyse the pre-event wetness state of soils in catchments. Within the summer months from



May to August for the period 1981 to 2020, selected parameters (cf. Sect. 2.3) were retrieved at a 1-hourly timestep. The horizontal grid spacing of the atmospheric data is $0.25^\circ \times 0.25^\circ$ and of the land data is $0.1^\circ \times 0.1^\circ$.

155 The *extreme precipitation event database* was created based on a processed version of the RADOLAN radar dataset from the German Weather Service (Weigl et al., 2004; Weigl and Winterrath, 2009; Winterrath et al., 2017). Data are available from 2001-2020 and were considered from May to August. The RADOLAN dataset has a 1x1 km grid size and a temporal resolution of 5 minutes. Although the original RADOLAN product is already quality checked and corrected and consequently reaching high quality, we applied some additional quality control and correction when needed. This included the detection and correction

160 of possible anomalous propagation (anaprop) echoes, further ground clutter detection and removal as well as an extended rain gauge adjustment with supplementary local rain gauges. Furthermore, the radar data were checked visually. We extracted the events for the database from the radar database by identifying 1x1 km grid cells with precipitation amounts $\geq 40 \text{ mm h}^{-1}$. This threshold was used according to the definition of extreme precipitation events by the German Weather Service (DWD, 2021). For every hour in which a grid cell exceeded the threshold, we extracted the maximum hourly precipitation sum as well as the

165 maximum 5-minute precipitation intensity. We selected an ERA5 grid cell as precipitation event if one or more high-resolution radar grid cells within the bigger, low-resolution ERA5 grid cell exceeded the hourly precipitation threshold. The final precipitation event database is therefore at the resolution of the ERA5 dataset including all events that were detected in the radar dataset.

The *flash flood database* was compiled via a search through scientific literature (Brauer et al., 2011; Bronstert et al., 2018; Van Campenhout et al., 2015; Eden et al., 2018; Göppert, 2018; Ruiz-Villanueva et al., 2012), water agency reports (Johst et al., 2018; Pfister et al., 2018, 2020), reinsurance data (Caisse Centrale de Réassurance (CCR), 2021), personal communication (engineering consultants Wald + Corbe) and news archives (Franceinfo, 2021; Luxemburger Wort, 2021). We included all floods in streams, fields or on streets that directly followed extreme convective precipitation. Despite a careful and comprehensive query, the database is likely non-exhaustive. A list of the events spanning the period from 1981 to 2020 can be

175 found in the Supplement S1 of this manuscript. To extract atmospheric parameters during flash flood events, we analysed hourly precipitation within the ERA5-grid cell of a specific event and its 8 neighbouring grid cells on the day of the flash flood. The maximum hourly precipitation value was considered the trigger for the flash flood and atmospheric parameters were extracted from the identified grid cell and time. For flash floods outside the temporal and spatial extent of the RADOLAN precipitation dataset, the exact timing of the flash flood event is unknown. Therefore, an occurrence time of 6 pm UTC was

180 taken, as we assume thunderstorms to occur most often in the evening hours (Van Delden, 2001).

2.3 Identification of atmospheric parameters favouring extreme precipitation and flash floods

Referring to work done by Van Delden 2001; Westermayer et al. 2017; Taszarek, Brooks, and Czernecki 2017; Púčik et al. 2015, we selected relevant atmospheric parameters to represent (1) instability, (2) the moisture content, and (3) the storm



185 motion. Additionally, we extracted (4) soil moisture content from the ERA5 dataset to get an indication for the wetness state
of the catchment before the onset of an extreme precipitation event (Table 1).

(1) As proxy parameters for atmospheric instability, we used the convective available potential energy (CAPE) [J kg^{-1}],
which is provided within the ERA5 single level datasets. In addition, we also considered convective inhibition (CIN)
[J kg^{-1}]. Given its recognised potential as flash flood proxy, we used the K-Index [$^{\circ}\text{C}$] that is provided within the
190 ERA5 dataset. The K-Index (George, 1960) is defined via Eq. (1) where T is the air temperature at differing pressure
levels and Td the dew point temperature in $^{\circ}\text{C}$.

$$K\text{-Index} = (T_{850 \text{ hPa}} - T_{500 \text{ hPa}}) + Td_{850 \text{ hPa}} - (T_{700 \text{ hPa}} - Td_{700 \text{ hPa}}) \quad (1)$$

The K-Index is a stability index, based on the vertical extent of low-level moisture and the vertical temperature lapse
rate of the lower and mid-troposphere. While the operational use of stability indices alone is limited (Doswell and
Schultz, 2006), indices can provide additional value when assessing severe weather potential. The K-Index was
195 originally developed to assess potential air mass thunderstorms, or thunderstorms without a dynamic triggering
mechanism (George, 1960). Most importantly, it shows some special skill in forecasting the potential of
thunderstorms related to heavy precipitation (Funk, 1991; Junker et al., 1999). Regarding the potential for heavy
precipitation, it can be generally stated that the higher the K-Index value, the greater the potential for heavy rain.
200 Originally, K-Index values above 20°C indicate thunderstorms, while there is no thunderstorm potential for values
below 20. K-Index values are further subcategorized into isolated thunderstorms ($20^{\circ}\text{C} - 25^{\circ}\text{C}$), widely scattered
thunderstorms ($25^{\circ}\text{C} - 30^{\circ}\text{C}$), scattered thunderstorms ($31^{\circ}\text{C} - 35^{\circ}\text{C}$) and numerous thunderstorms ($> 35^{\circ}\text{C}$). Note
that the highest category with K-Index values above 35°C is however extremely rare in central western Europe.

(2) To reach a sufficiently high rainfall rate causing heavy precipitation and consequent flash floods, the atmosphere's
205 moisture content is pivotal. We opted for the total column water vapour (TCWV) [kg m^{-2}] as well as specific humidity
(q) [kg kg^{-1}] and relative humidity (RH) [%] at the pressure level of 700 hPa as atmospheric moisture content proxies.

(3) To assess the storm motion, we computed the wind speed (WS) from the square root of the squared northward
direction wind vector u [m s^{-1}] and the squared eastward direction wind vector v [m s^{-1}] at the pressure level of 700
hPa. Low-level wind shear (LLS) [m s^{-1}] was likewise computed based on the square root of the differences of the
210 vectors u and v at pressure levels at ground (1000 hPa) and at about 1 km height levels (850 hPa). Accordingly, we
calculated the deep-layer wind shear (DLS) [m s^{-1}] as the difference of the wind vectors at ground (1000 hPa) and in
about 6 km height levels (500 hPa). The wind shear allows an assessment of the organisational mode of deep moist
convection.

(4) We considered soil moisture parameters for assessing the pre-event wetness state of a catchment. Therefore, we
215 extracted soil moisture (Swvl) [$\text{m}^3 \text{m}^{-3}$] at depths of 0-7 cm, 7-28 cm, and 28-100 cm from ERA5, 24 hours before
identified events.



Table 1: Selected proxy parameters for the assessment of convection relevant atmospheric conditions from the ERA5 dataset.

Proxy for	Parameter	Abbr.	Unit	Level	Source
Instability	Convective available potential energy	CAPE	J kg ⁻¹	single	Hersbach et al., 2018b
	Convective inhibition	CIN	J kg ⁻¹	single	Hersbach et al., 2018b
	K-Index	Kx	°C	single	Hersbach et al., 2018b
Moisture	Total column water vapour	TCWV	kg m ⁻²	single	Hersbach et al., 2018b
	Specific humidity	q	kg kg ⁻¹	700 hPa	Hersbach et al., 2018a
	Relative humidity	RH	%	700 hPa	Hersbach et al., 2018a
Storm motion	U-component of wind	u	m s ⁻¹	700 hPa	Hersbach et al., 2018a
	V-component of wind	v	m s ⁻¹	700 hPa	Hersbach et al., 2018a
Catchment wetness state	Volumetric soil water layer 1	Swvl1	m ³ m ⁻³	0-7 cm	Muñoz Sabater, 2019
	Volumetric soil water layer 2	Swvl2	m ³ m ⁻³	7-28 cm	Muñoz Sabater, 2019
	Volumetric soil water layer 3	Swvl3	m ³ m ⁻³	28-100 cm	Muñoz Sabater, 2019

220 To identify extreme precipitation and flash flood relevant proxy parameters, we extracted their respective values from the ERA5 atmospheric dataset at the time step and grid cell of initially identified events. Next, we created thresholds for every proxy parameter, that make the occurrence of precipitation events possible. Therefore, we chose upper or lower boundaries including 75 % of extreme events. This analysis leads to the determination of the thresholds in Table 2, Sect. 3.3, to classify atmospheric conditions as extreme precipitation and potentially flash flood favouring. We used these thresholds, as well as the three parameters identified the most suitable from the groups of moisture, instability, and storm motion to eventually conduct trend analyses.

2.4 Trend analyses

We carried out linear trend analyses to prove the different parts of our working hypothesis – linking a potential increase in atmospheric conditions triggering extreme precipitation events to a rise in the occurrence of flash flood events in central western Europe. We applied the linear models to our flash flood database, as well as to the occurrence frequency, precipitation amount and maximum 5-minute intensity of identified extreme precipitation events. Likewise, we applied linear models to the flash flood relevant parameter ranges of the identified set of ERA5 atmospheric parameters, as well as to the simultaneous occurrences of the three most relevant parameters.



3 Results

235 3.1 More frequent flash floods

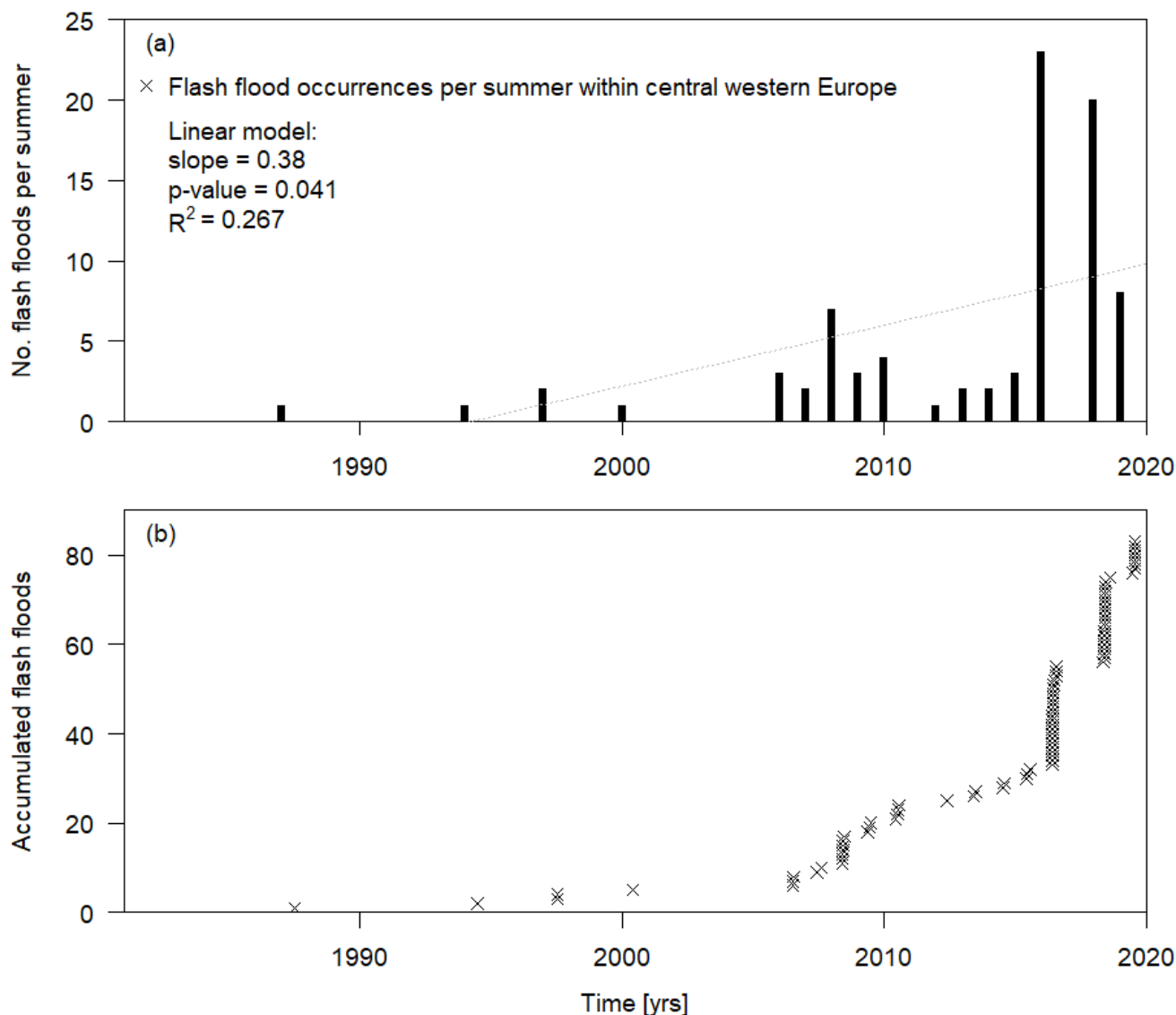


Figure 2: Occurrence of flash flood events within central western Europe between 1981 and 2020. Panel (a) shows the number of flash flood occurrences per year, panel (b) maintains the exact occurrence date of the flash flood event.

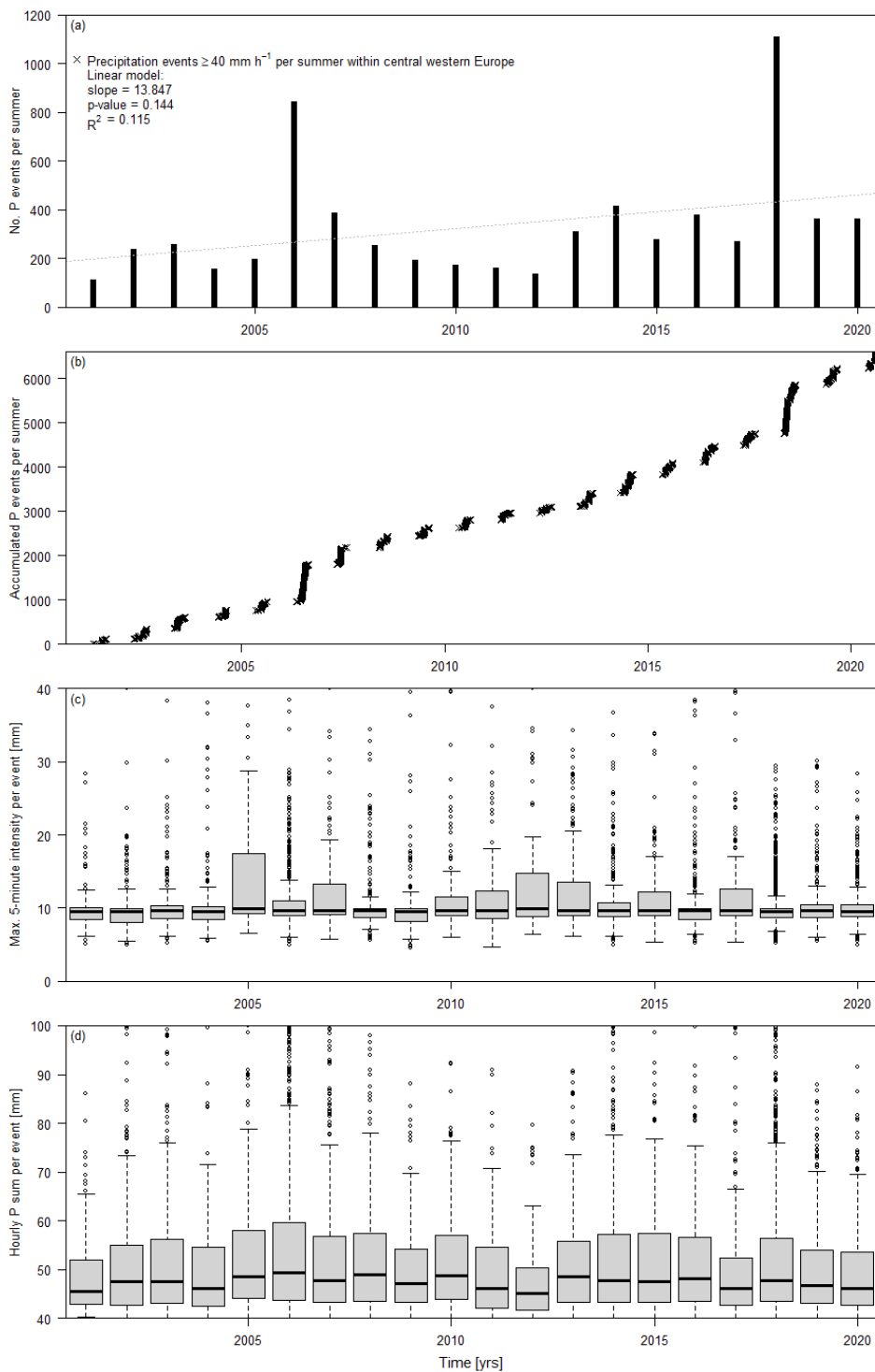
The patterns of flash flood occurrence in central western Europe have substantially changed between 1981 and 2020 (Figure 2 (a)). A simple linear model applied to the number of annual flash floods shows an increasing trend of 0.382 events per year (p-value 0.039). While barely any events were reported before 2006, two remarkable years are 2016 and 2018, when flash floods occurred particularly often in the study area (23 and 20 occurrences respectively). Possibly, there might be a breakpoint



in the time series before 2016. This can however not be demonstrated statistically as the time series after 2016 is still too short. Note that often several events occurred within a few days (Figure 1 (b)) under the same meso-scale atmospheric constellation, in the same area or even in neighbouring catchments, and are, therefore, not independent from one another.

3.2 Unchanged occurrence of extreme precipitation events

Within our study area, we extracted extreme precipitation events with precipitation sums $\geq 40 \text{ mm h}^{-1}$ from the DWD-radar-dataset. Between 2001 and 2020, we observed a slight increase in the number of events per year (Figure 3a). Note that interannual variance is very high and that this increase includes two extreme years, 2006 and 2018, when precipitation events $\geq 40 \text{ mm h}^{-1}$ occurred particularly often. Similar to the flash flood occurrences, many of the extreme precipitation events happened on the same days over a wider region. This is particularly the case for 2008 and 2018 (Figure 3b) – with the multiple rainfall events from 2018 overlapping with a high number of flash floods. For the precipitation amounts we could not find significant trends in the 2001-2020 period for both the maximum 5-minute intensity (Figure 3c) and the hourly precipitation sums per event (Figure 3d).



255

Figure 3: Occurrence of extreme precipitation events ($\geq 40 \text{ mm h}^{-1}$) within central western Europe.



3.3 Identification of atmospheric parameters favouring extreme precipitation and flash flood events

To identify parameter ranges that favour flash floods, we considered all hourly values, as well as the parameters present during the time of extreme precipitation events and the selection of precipitation events that led to flash flood occurrences (Figure 4).

260 The data emphasise the occurrence of extreme events under conditionally unstable atmospheric conditions. Most extreme precipitation and flash flood events occurred within the upper quartile of CAPE values (Figure 4a). High values of CAPE are often accompanied by low values of CIN. While extreme precipitation events occurred over a wide range of CIN, CIN is mostly limited to values below 100 J kg^{-1} during flash flood events (Figure 4b). However, both CAPE and CIN appear to be widely scattered within the upper and respectively lower spectrum of their possible ranges. The K-Index, in contrast, proves

265 to be a reliable index and more than 80 % of all extreme precipitation and flash flood events occur within the thunderstorm relevant categories of the index above 20°C (Figure 4c). Moisture conditions during extreme precipitation and flash flood events were found to be mostly within the upper percentiles of the overall simulated values. Especially the specific humidity (q) during events ranges clearly within the upper quartile of all values (Figure 4e). Total column water vapour (TCWV) and relative humidity (RH) also prove to always be high during extreme events. All moisture parameters, and especially RH tend

270 to be even higher during flash flood events compared to general extreme precipitation events (Figure 4d-f). The wind related parameters considered to analyse storm motion and organisation are generally low during extreme precipitation and flash flood events. Especially the wind speed (Figure 4g) and DLS (Figure 4i) stand out, with most of the values observed during extreme events being in the lower quartile of the full range of occurrences. Tendencies regarding LLS (Figure 4k) are less clear but show the same pattern. In addition to atmospheric parameters, soil moisture conditions were evaluated 24 h before identified

275 events. Often, soil moisture within the upper and lower soil layer ($\text{Swv1}_{0-7 \text{ cm}}$, $\text{Swv1}_{37-100 \text{ cm}}$) is higher during flash flood events compared to general extreme precipitation events (Figure 4j, l). The mid-level soil layer ($\text{Swv1}_{27-28 \text{ cm}}$) does not show major differences before flash flood events (Figure 4k).

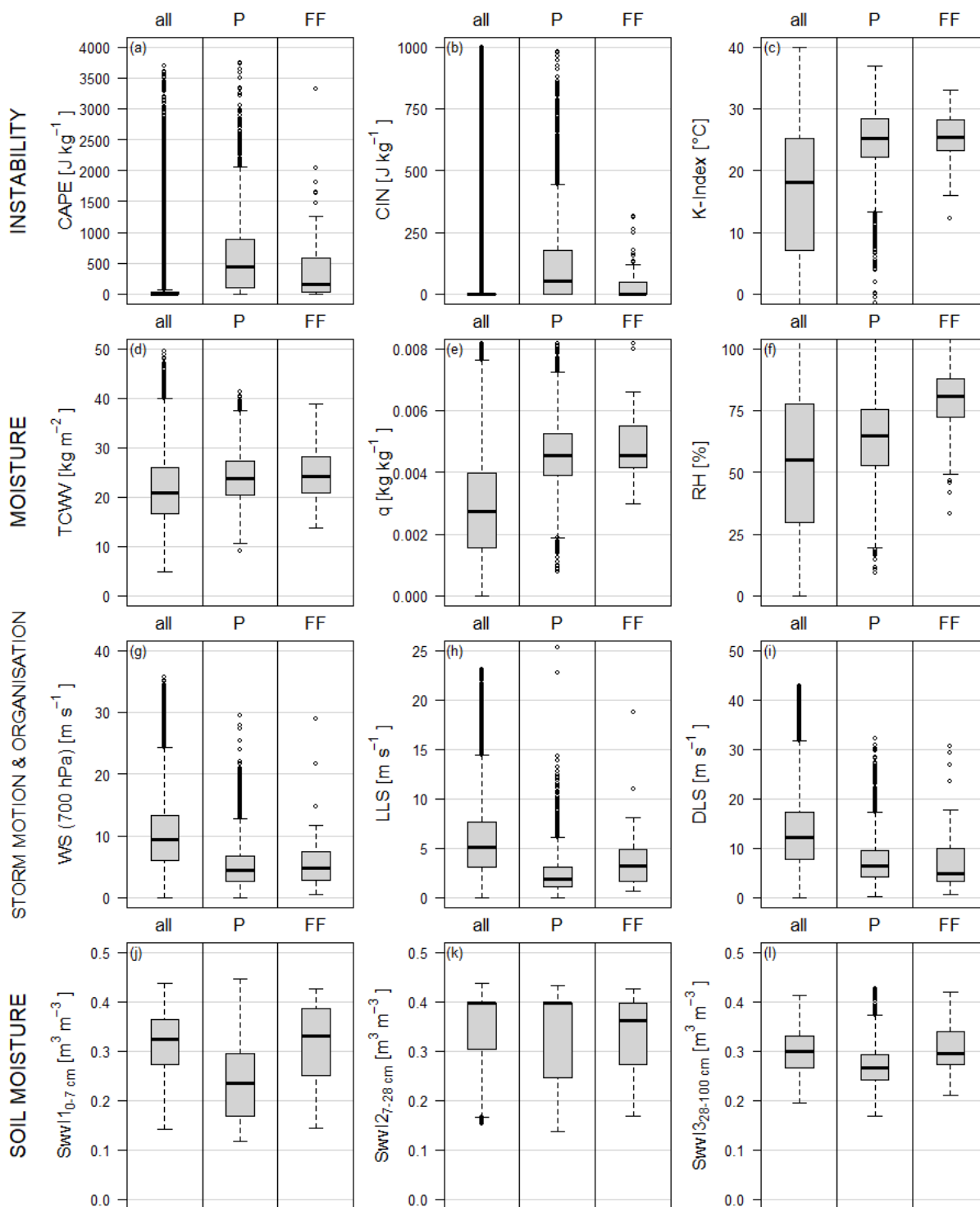


Figure 4: All hourly values of the proxy parameters (a-i) during the entire time period (all), during extreme precipitation events (P) and before flash flood events (FF). Soil moisture (j-l) was extracted 24 hours before identified P or FF events.



285

This analysis leads to the determination of the thresholds in Table 1 to classify atmospheric conditions as extreme precipitation and potentially flash flood favouring. Moreover, high CAPE, high q and weak DLS were identified as the most clearly distinguishing parameters per category to characterize extreme precipitation events, including 75 % of all extreme precipitation events and excluding 75 % of all generally occurring parameters values.

Table 2: Threshold values determined as flash flood favouring based on the lower/upper quartile of their range of occurrence during extreme precipitation events.

Instability			Moisture			Storm motion & organisation			Soil moisture		
CAPE	CIN	Kx	TCWV	q	RH	WS	LLS	DLS	Swv11	Swv12	Swv13
≥ 100	≤ 180	≥ 22	≥ 20	≥ 0.004	≥ 50	≤ 7	≤ 3	≤ 10	No threshold defined		
J kg^{-1}	J kg^{-1}	$^{\circ}\text{C}$	kg m^{-2}	kg kg^{-1}	%	m s^{-1}	m s^{-1}	m s^{-1}	$\text{m}^3 \text{m}^{-3}$		

3.4 Changes of atmospheric parameters between 1981-2020

Instability, as shown representatively by CAPE above 100 J kg^{-1} , has increased between 1981 and 2020. The number of hours with high enough instabilities to support the occurrence of thunderstorms increased by up to five hours per year (Figure 5a). These findings were particularly significant for the northern part of the study area (Figure 5b). There are however no clear trends regarding the actual values of CAPE above 100 J kg^{-1} (Figure 5c, d).

The observed increase in high atmospheric moisture content, represented by specific humidity above 0.004 kg kg^{-1} (Figure 5e, g), is highly significant over the entire study area (Figure 5f, h). Conditions with high moisture content became up to 8 hours per year more frequent, especially over south-western Germany. The absolute increase of very high moisture content is however small (Figure 5g).

The storm motion potentially decreases with weak DLS that tends to occur more often over most parts of the study area (Figure 5i). The values below the threshold of 10 m s^{-1} appear to become higher in the western part of the study area and lower within the eastern part. These trends are however insignificant over the entire study area (Figure 5j, l) and DLS is considered to remain largely unchanged.

The complete set of analysed atmospheric parameters is shown in Appendix A.

300

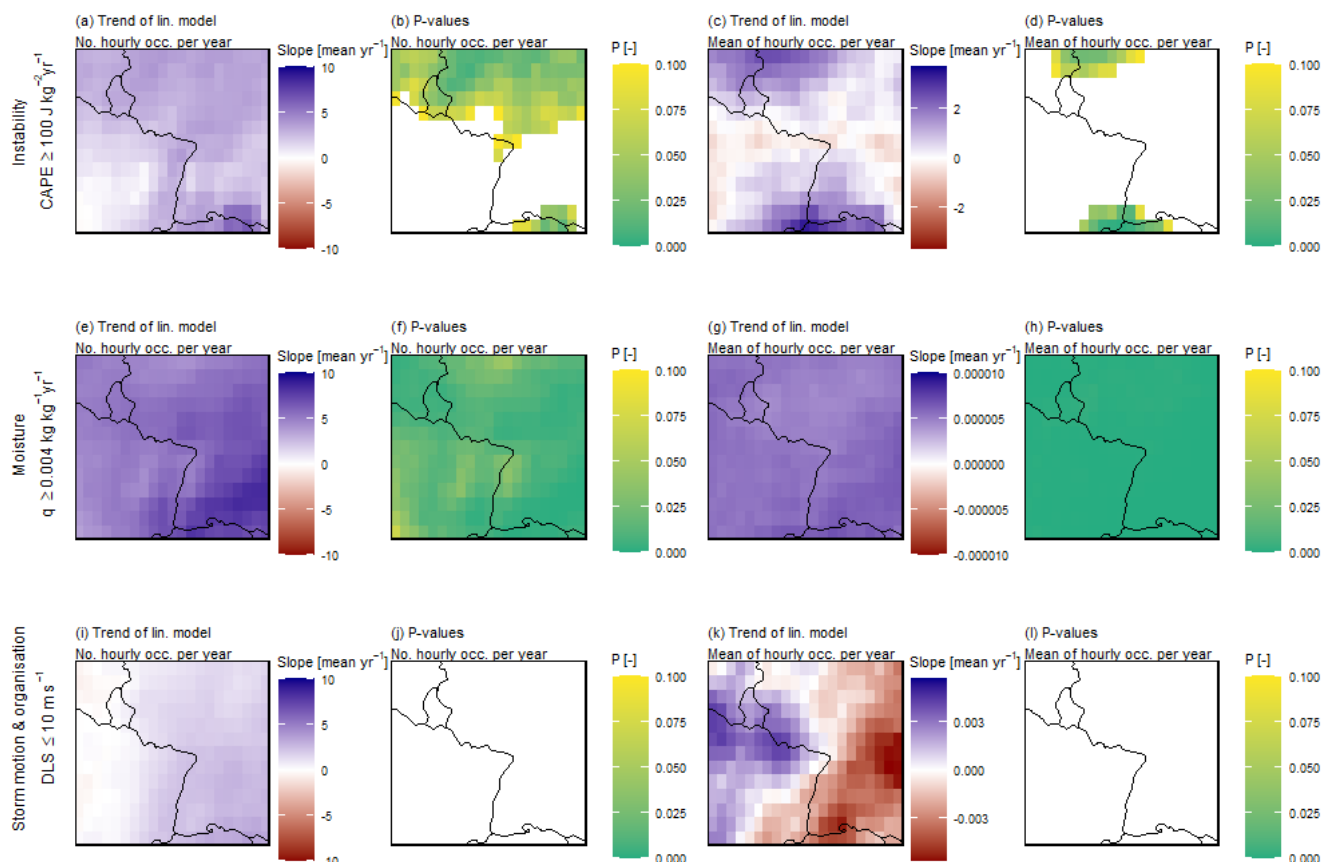
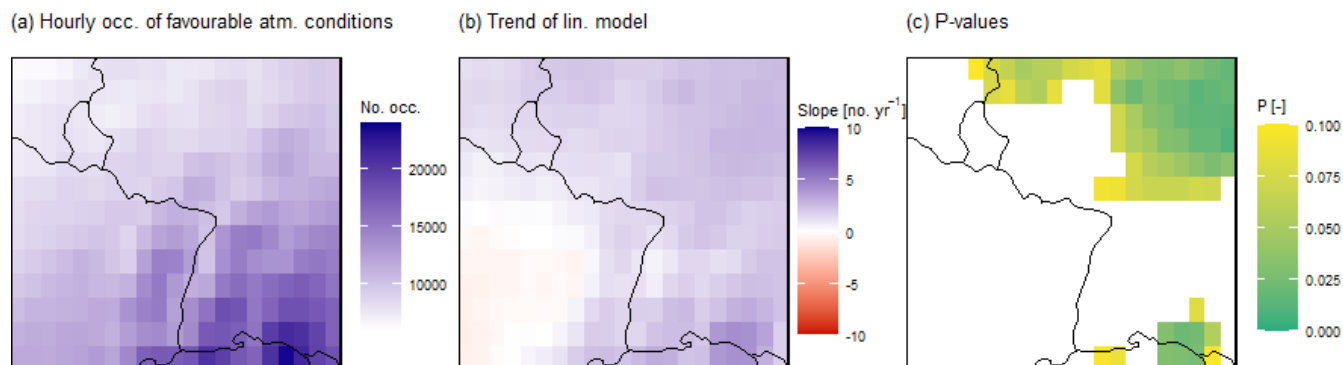


Figure 5: Trend analysis of the most suitable variables for instability (CAPE), moisture (specific humidity q), and storm motion and organisation (DLS). The first column (a, e, i) shows the trends of the numbers of hourly occurrences of values above their respective threshold, including their significance-levels p in the second column (b, f, j). The third column (c, g, k) shows the trends of the mean values of all hourly occurrences above the threshold and the last column (d, h, l) their respective significance-levels p . White areas mark insignificance.

3.5 Spatial distribution of atmospheric conditions favouring extreme precipitation and flash flood events

The simultaneous occurrence of the three most characteristic identified atmospheric parameters from each component (CAPE, q , DLS) within extreme event favouring parameter ranges is correlated with topography (Figure 1c). Favourable atmospheric conditions occur most frequently over the Vosges Mountains in France and in south-western Germany, compared to the rest of the study area. Over eastern Belgium, favourable atmospheric conditions have occurred less than half as often between 1981 and 2020 (Figure 6a). Within this period, the occurrence of favourable atmospheric conditions changed very little. Over south-western Germany, the simultaneous occurrence of these three parameters occurred only 1-2 h per year more often, while over north-eastern France these conditions occur slightly less often (Figure 6b). The significance of these combinations is however low. (Figure 6c).



320 **Figure 6:** Panel (a) shows the overall number of hourly occurrences of atmospheric conditions favouring extreme precipitation and flash flood events during the summer months between 1981 and 2020. Panel (b) illustrates the positive trends of atmospheric conditions favouring extreme precipitation and flash flood events per year, and panel (c) the significance of the linear model. White areas mark insignificance.

4 Discussion

The compiled database shows an increase in flash floods occurrences in temperate central western Europe between 1981 and 2020. Barely any events were found in the two first decades. This increase is further supported by the recently increasing number of reports and scientific publications on the topic (e.g. Bronstert et al., 2018; Van Campenhout et al., 2015; Marchi et al., 2010; Ruiz-Villanueva et al., 2012). In a wider context, these flash floods might even be seen as an extension of the continental “flash flood belt” ranging from the Black Sea via Slovakia, Slovenia, northern Italy, and Austria, to south-western Germany and now potentially extending into Luxembourg (Marchi et al., 2010; Ruiz-Villanueva et al., 2012). Furthermore, this increase is in line with similar observations in the Mediterranean area (Llasat et al., 2016) and lowland catchments of Alpine regions (Sikorska-Senoner and Seibert, 2020). However, as per their nature, flash floods are rare phenomena. Therefore, we categorized a wide range of floods triggered by thunderstorms as flash floods. Yet, uncertainties about their precise spatial and temporal distribution remain. Beyond that, the method of data collection is influenced by the progress of digitalisation which might make recent years appear more often in search engines. Additionally, we browsed through historical archives but did not find further entries. Note, that the trend we identified is strongly influenced by two years in which especially many events occurred: 2016 and 2018 (and possibly the July 2021 floods, that were not considered in this manuscript but may further strengthen the increasing trend). During these event series, atmospheric conditions were characterised by exceptionally long-lasting weather patterns associated with very moist and unstable air masses. These conditions led to the extraordinary high number and severity of thunderstorms with substantial flooding in central western Europe (Mohr et al., 2020; Piper et al., 2016).

340 Based on the DWD’s RADOLAN dataset we were not able to detect any linear trends in the number of precipitation events per year, their hourly sums or their maximum 5-minute intensity between 2002-2020. These findings are in line with similar analyses done by the DWD and GDV (2019). As the detection of extreme precipitation events remained challenging due to



their localised occurrence, large-scale data were only available through the deployment of a dense radar station network as of 2002. Note that this observation period remains rather short and does not allow to infer solid conclusions on potential trends. Also, while weather radars provide precipitation data of high spatial resolution, various sources of uncertainty may prevail –
345 related to precipitation type and intensity, topography, distance to the radar source, etc. (Meischner, 2014; Strangeways, 2007; Winterrath et al., 2017). We accounted for some of these potential effects (e.g., rain gauge adjustments, detection, and correction of possible anomalous propagation echoes). Perhaps, trends in extreme precipitation events could be detected when considering preceding decades as well. Müller and Pfister (2011) analysed longer time series starting in 1980 and indeed found an increase in intense rainstorms during summer months in western Germany (Emscher-Lippe catchment). However,
350 precipitation generally varies considerably on an interannual basis and makes trend analyses challenging.

We found that atmospheric conditions favouring extreme precipitation and subsequent flash flood events became slightly more frequent and intensities of relevant atmospheric parameters increased. The most significant increases were found for the moisture parameters. Both, TCWV and q , increased significantly over central western Europe indicating potentially higher precipitation amounts. Yet, rising air temperatures inhibit an increase in higher RH (Rädler et al., 2018). The increase of q also
355 influences instability parameters, such as CAPE and the K-Index, to increase at a significant level in some areas. This matches well with the findings by Taszarek et al. (2021b) who documented an increase of CAPE over central Europe. Trends of CIN are however ambiguous within the same period. While in some areas favouring conditions do occur more often, there are indications that CIN increases as well. This increase in CIN might offset some of the instability increases through CAPE (Taszarek et al., 2021a). In this study, we did not analyse the simultaneous occurrences of CAPE and CIN in detail, but Chen
360 et al. (2020) found highly complex interactions, suggesting that future moist convection and rainstorms may become less frequent but more intense. Regarding low wind speeds and weak bulk shear, we found slightly increasing but barely significant trends. Therefore, the organisation and motion of storm systems stayed largely unchanged. Studies looking at substantial DLS for other convective hazards such as hail or tornadoes did not identify significant trends either (Púčik et al., 2017; Rädler et al., 2018). Wind speed and shear are not directly relevant for triggering precipitation but slightly increasing the duration of an
365 event, they are potentially contributing to the development of flash floods. The coarse resolution of the ERA5 atmospheric data might miss smaller-scale wind features related to orography. Even though extreme precipitation and flash floods tend to occur locally, they happen during meso- to large-scale favouring conditions, which should be well captured by the reanalysis data.

The values of the considered atmospheric parameters cover the expected ranges of occurrence. However, to include 75 % of
370 all precipitation and flash flood events, we had to include an even wider parameter range. This holds especially true for the lower and respectively upper thresholds of CAPE and CIN, that appear low and respectively high compared to common values present during thunderstorms (Púčik et al., 2015; Taszarek et al., 2017). In the ERA5 data, both parameters showed an extremely high variability in space and time. As for our identified events we found that CAPE, as well as CIN, were often higher and respectively lower in a neighbouring grid cell or time step, compared to the grid cell and time step in which we



375 identified most rain. This variability of CAPE also leads to a relatively low number of hours with all parameters within their ranges, as shown in Sect. 3.5 (Figure 6).

The focus of our work was the attempt to link atmospheric conditions, extreme precipitation and flash floods: The observed increase in flash floods is a consequence of more intense or more often occurring precipitation events, that are initiated by thunderstorm favouring atmospheric conditions. However, reality seems a lot more complex. While atmospheric conditions
380 tend to become more unstable, and overall warmer air masses potentially possess a higher amount of water vapour, the expected increase in (convective) precipitation events were not obvious from the analysed data. Thus, the increase in flash flood occurrences cannot be explained by the sole increase in precipitation intensity or occurrence frequency.

Other factors than those that we have considered in this study may influence the development of flash floods. One could be the duration of favouring atmospheric conditions. Both remarkable flash flood series from 2016 and 2018 occurred during
385 atmospheric blocking situations (Mohr et al., 2020; Piper et al., 2016) that stymied the movement of the atmosphere, ultimately causing weather constellations to last longer and thus creating extreme situations. In recent years they have been increasingly observed, especially in summer (Detring et al., 2021; Lupo, 2020). This could hint to a change in the intra-annual distribution of precipitation, while the number of precipitation events, their maximum 5-minute intensity, and their hourly sum stayed – apart from their large intra-annual variations – at a similar level between 2001 and 2020. Sequences with abundant rainfall
390 may eventually rise a catchment's soil moisture and accelerate the development of a flood event. Flash floods in continental regions mostly occur when soil moisture is high at the onset of an event (Marchi et al., 2010; Pfister et al., 2020). Moreover, catchment-specific parameters such as topography, land use, soil properties, geology or other factors may equally impact the development of flash floods (Marchi et al., 2010).

5 Conclusion

395 The goal of this study was to investigate the causes for a more frequently observed flash floods in temperate regions of central western Europe. For this purpose, we compiled a flash flood database based on scientific literature, water agency data and the information of local consultants and analysed it using linear regression models. For the identification of extreme precipitation events potentially triggering flash floods, we relied on a 5-minute radar dataset (RADOLAN, DWD) and analysed all events exceeding the threshold of 40 mm h^{-1} statistically considering hourly precipitation sums as well as 5-minute maxima. The
400 identified flash flood and precipitation events were then connected to convection relevant atmospheric parameters of the ERA5 reanalysis dataset representing instability, moisture content and system motion and organisation. We leveraged these data for testing our hypothesis that a change in atmospheric conditions led to more frequent extreme precipitation events that subsequently led to more flash flood events in central western Europe.. We tested our hypothesis in three steps:

405 I) The hypothesised increase in the occurrence of flash floods was confirmed, despite possible minor biases in the database.



- II) An increase in the frequency and intensity of extreme precipitation events could not be confirmed with the available database and analysis due to a large interannual variation in events. Future analyses could incorporate the intra-annual temporal distribution of extreme precipitation events. Perhaps, formerly evenly distributed rainfall events tend to occur more condensed within a few days.
- 410 III) Via proxy parameters we did find changes in the occurrence of atmospheric conditions favouring extreme precipitation and flash flood events. High absolute moisture content (q , TCWV) has increased between 1981 and 2020, while RH decreased slightly. Proxy parameters representing sufficient instability (CAPE, K-Index) increased as well and so did CIN, which might oppose some of the instability gains of CAPE (Taszarek et al., 2021a). Parameters determining weak storm motion and organisation (WS, DLS) did not show significant changes, but the occurrence of
- 415 weak LLS increased slightly. Overall, the most important components favouring flash flood relevant atmospheric conditions, abundant moisture and sufficient latent instability, have become more frequent and higher values indicate possibly more severe events.

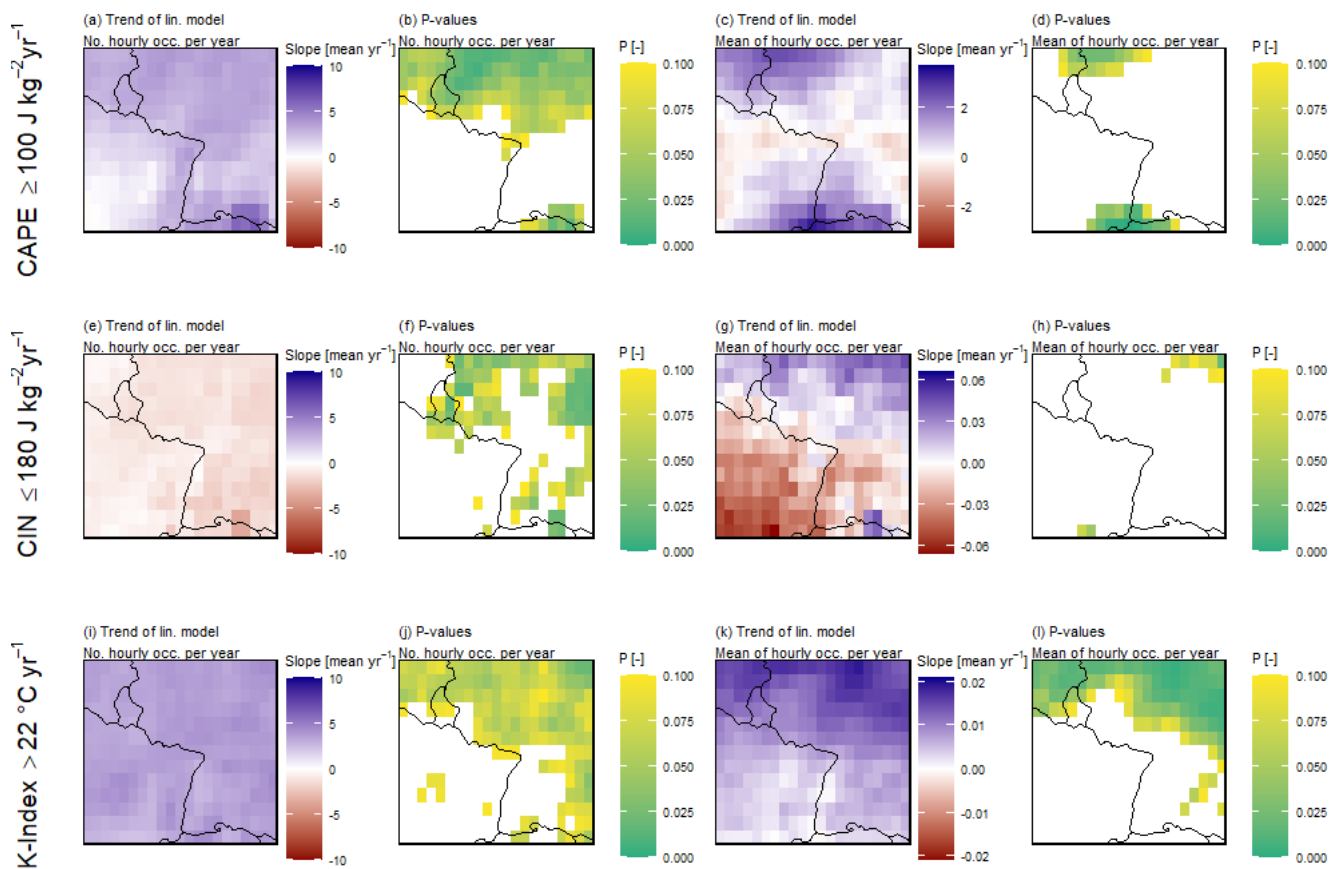
Consequently, the sub-hypotheses I and III are confirmed, while the second sub-hypothesis was rejected. Hence, the simple causal chain between the atmospheric conditions, extreme precipitation and flash floods assumed in the overarching hypothesis

420 does not do justice to the entire complexity of problems. Interconnections seem far more complex than hypothesised. In addition to the hypothesis, we found mostly higher upper (0-7 cm) and lower (28-100 cm) layer soil moisture during flash flood events compared to general extreme precipitation events. These results might point us in other directions, possibly to changes in intra-annual temporal patterns of rainfall and consequently different pre-event soil moisture conditions. Another explanation might be non-atmospheric, catchment-specific parameters, that were not considered in this study.

425 To the best of our knowledge, this work is none the less among the first ones focussing on the convective hazard of extreme precipitation that was often neglected, giving priority to hail or tornadoes. As extreme precipitation is extremely variable in space and time and can derive from many different weather constellations, it remains a challenge to pinpoint atmospheric conditions that trigger them. This makes possible assumptions about the future extremely challenging.

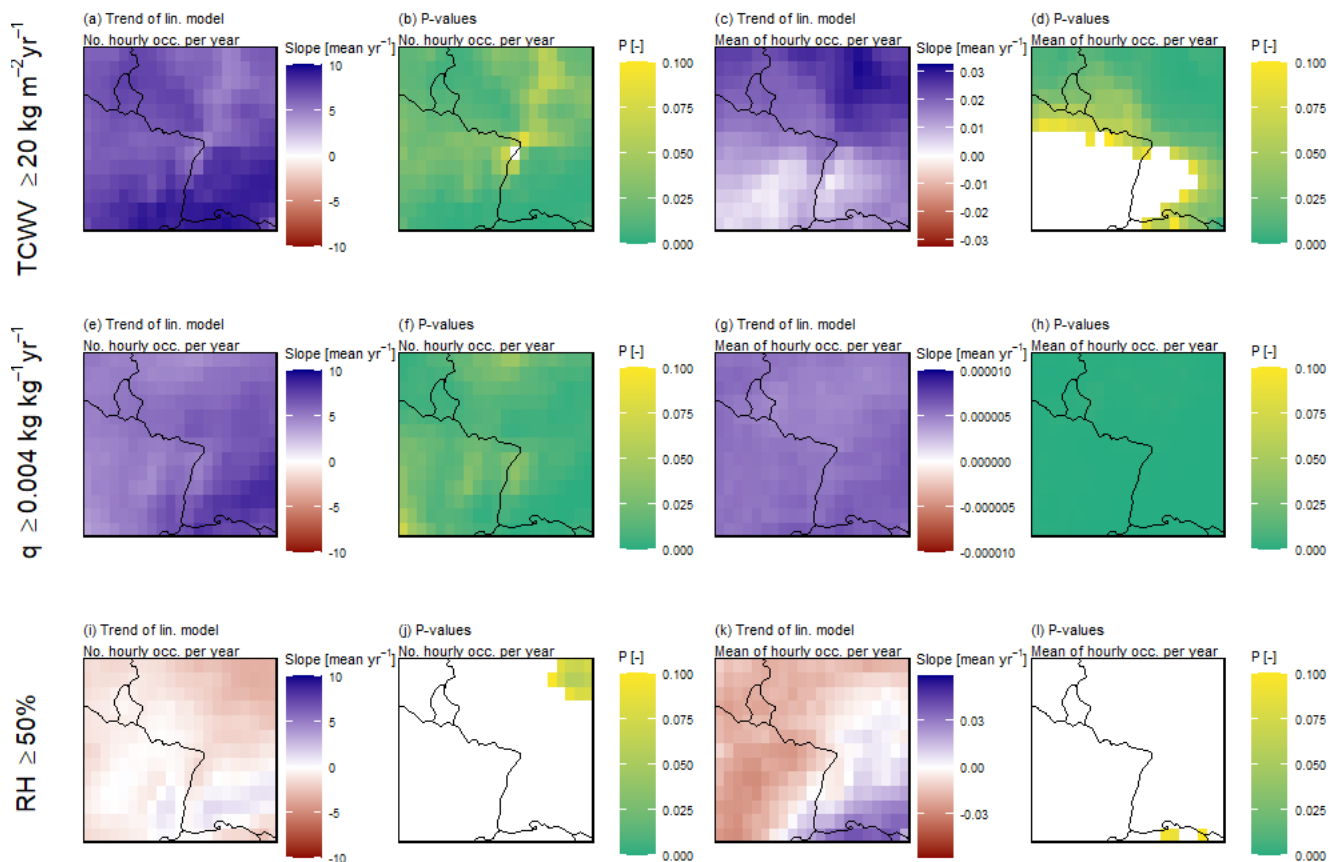


Appendix A : Spatial trends of atmospheric parameters within central western Europe



430

Figure A1: Trend analysis of the three variables for instability (CAPE, CIN, K-Index). The first column (a, e, i) shows the trends of the numbers of hourly occurrences of values above their respective threshold, including their significance-levels p in the second column (b, f, j). The third column (c, g, k) shows the trends of the mean values of all hourly occurrences above the threshold and the last column (d, h, l) their respective significance-levels p. White areas mark insignificance.



435

Figure A2: Trend analysis of the three variables for moisture (TCWV, q , RH). The first column (a, e, i) shows the trends of the numbers of hourly occurrences of values above their respective threshold, including their significance-levels p in the second column (b, f, j). The third column (c, g, k) shows the trends of the mean values of all hourly occurrences above the threshold and the last column (d, h, l) their respective significance-levels p . White areas mark insignificance.

440

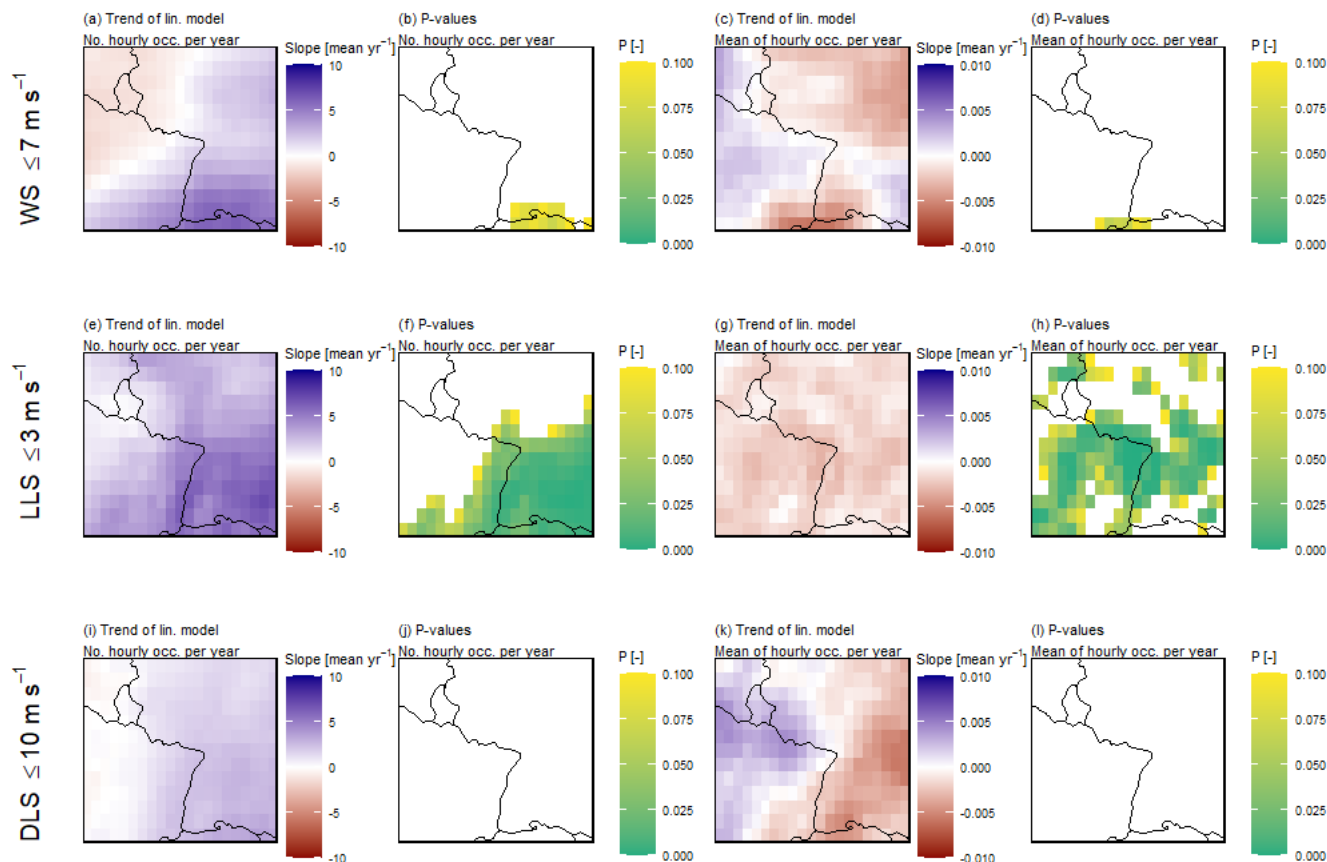


Figure A3: Trend analysis of the three variables for storm motion and organisation (WS, LLS, DLS). The first column (a, e, i) shows the trends of the numbers of hourly occurrences of values above their respective threshold, including their significance-levels p in the second column (b, f, j). The third column (c, g, k) shows the trends of the mean values of all hourly occurrences above the threshold and the last column (d, h, l) their respective significance-levels p . White areas mark insignificance.

445

Data availability

The flash flood database used in this manuscript is added to the supplements. The RADOLAN radar dataset by the German Weather Service (DWD) is free for download from their open data server [https://opendata.dwd.de/climate_environment/CDC/grids_germany/5_minutes/radolan/reproc/2017_002/, last accessed June 2021]. The ERA5 atmospheric parameters are also free for download from the Climate Data Store (CDS) of the Copernicus Climate Change Service (C3S) [https://cds.climate.copernicus.eu, last accessed November 2021].

450



Author contributions

JM, MN, LP, and LM conceptualized the study. JM collected the flash flood and ERA5 data, carried out the analysis and wrote
455 the first draft of the manuscript. MN provided the processed precipitation radar data. All co-authors (JM, MN, LP, LM, EZ)
contributed to and edited the manuscript.

Competing interests

The authors declare that they have no conflict of interest.

Acknowledgements

460 This work is supported by the Luxembourg National Research Fund (FNR) via the PRIDE programme for doctoral education
(grant PRIDE15/10623093/HYDRO-CSI). We also acknowledge all data source providers for this work: The German Weather
Service (DWD) for the RADOLAN radar data, the Copernicus Climate Change Service for the ERA5 dataset as well as
Catharin Schäfer and Dr. Hans Göppert from the engineering consultant Wald + Corbe for providing their collection of flash
flood events.

465 References

- Alfieri, L., Smith, P. J., Thielen-Del Pozo, P. J. and Beven, K. J.: A staggered approach to flash flood forecasting - Case study
in the Cévennes region, *Adv. Geosci.*, 29, 13–20, doi:10.5194/adgeo-29-13-2011, 2011.
- Bertola, M., Viglione, A., Lun, D., Hall, J. and Blöschl, G.: Flood trends in Europe: Are changes in small and big floods
different?, *Hydrol. Earth Syst. Sci.*, 24(4), 1805–1822, doi:10.5194/hess-24-1805-2020, 2020.
- 470 Bertola, M., Viglione, A., Vorogushyn, S., Lun, D., Merz, B. and Blöschl, G.: Do small and large floods have the same drivers
of change? A regional attribution analysis in Europe, *Hydrol. Earth Syst. Sci.*, 25(3), 1347–1364, doi:10.5194/hess-25-1347-
2021, 2021.
- Borga, M., Boscolo, P., Zanon, F. and Sangati, M.: Hydrometeorological analysis of the 29 August 2003 flash flood in the
eastern Italian Alps, *J. Hydrometeorol.*, 8(5), 1049–1067, doi:10.1175/JHM593.1, 2007.
- 475 Brauer, C. C., Teuling, A. J., Overeem, A., van der Velde, Y., Hazenberg, P., Warmerdam, P. M. M. and Uijlenhoet, R.:
Anatomy of extraordinary rainfall and flash flood in a Dutch lowland catchment, *Hydrol. Earth Syst. Sci.*, 15, 1991–2005,
doi:10.5194/hess-15-1991-2011, 2011.
- Bronstert, A., Agarwal, A., Boessenkool, B., Fischer, M., Heistermann, M. and Köhn-Reich, L.: Die Sturzflut von Braunsbach
am 29. Mai 2016 – Entstehung, Ablauf und Schäden eines „Jahrhundertereignisses“. Teil 1: Meteorologische und
480 hydrologische Analyse, *Hydrol. und Wasserbewirtschaftung*, 61, 150–162, doi:10.5675/HyWa, 2017.



- Bronstert, A., Agarwal, A., Boessenkool, B., Crisologo, I., Fischer, M., Heistermann, M., Köhn-Reich, L., López-Tarazón, J. A., Moran, T., Ozturk, U., Reinhardt-Imjela, C. and Wendi, D.: Forensic hydro-meteorological analysis of an extreme flash flood: The 2016-05-29 event in Braunsbach, SW Germany, *Sci. Total Environ.*, 630, 977–991, doi:<https://doi.org/10.1016/j.scitotenv.2018.02.241>, 2018.
- 485 Brooks, H. E.: Proximity soundings for severe convection for Europe and the United States from reanalysis data, *Atmos. Res.*, 93(1–3), 546–553, doi:[10.1016/j.atmosres.2008.10.005](https://doi.org/10.1016/j.atmosres.2008.10.005), 2009.
- Bucala-Hrabia, A., Kijowska-Strugała, M., Bryndal, T., Cebulski, J., Kiszka, K. and Krocak, R.: An integrated approach for investigating geomorphic changes due to flash flooding in two small stream channels (Western Polish Carpathians), *J. Hydrol. Reg. Stud.*, 31, 100731, doi:[10.1016/j.ejrh.2020.100731](https://doi.org/10.1016/j.ejrh.2020.100731), 2020.
- 490 Caisse Centrale de Réassurance (CCR): Événements - inondations, Paris. [online] Available from: <https://catastrophes-naturelles.ccr.fr/les-evenements>, 2021.
- Van Campenhout, J., Hallot, E., Houbrechts, G., Peeters, A., Levecq, Y., Gérard, P. and Petit, F.: Flash floods and muddy floods in Wallonia: Recent temporal trends, spatial distribution and reconstruction of the hydrosedimentological fluxes using flood marks and sediment deposits, *Belgeo*, 1, 0–26, doi:[10.4000/belgeo.16409](https://doi.org/10.4000/belgeo.16409), 2015.
- 495 Chen, J., Dai, A., Zhang, Y. and Rasmussen, K. L.: Changes in convective available potential energy and convective inhibition under global warming, *J. Clim.*, 33(6), 2025–2050, doi:[10.1175/JCLI-D-19-0461.1](https://doi.org/10.1175/JCLI-D-19-0461.1), 2020.
- Van Delden, A.: The synoptic setting of thunderstorms in Western Europe, *Atmos. Res.*, 56(1–4), 89–110, doi:[10.1016/S0169-8095\(00\)00092-2](https://doi.org/10.1016/S0169-8095(00)00092-2), 2001.
- Detring, C., Müller, A., Schielicke, L., Névir, P. and Rust, H. W.: Occurrence and transition probabilities of omega and high-
500 over-low blocking in the Euro-Atlantic region, *Weather Clim. Dyn.*, 2, 927–952, doi:<https://doi.org/10.5194/wcd-2-927-2021>, 2021.
- Doswell, C. A. and Schultz, D. M.: On the use of indices and parameters in forecasting severe storms, *E-Journal Sev. Storms Meteorol.*, 1(3), 1–22, 2006.
- Doswell, C. A., Brooks, H. E. and Maddox, R. A.: Flash flood forecasting: An ingredients-based methodology, *Weather
505 Forecast.*, 11(4), 560–581, doi:[10.1175/1520-0434\(1996\)011<0560:FFFAIB>2.0.CO;2](https://doi.org/10.1175/1520-0434(1996)011<0560:FFFAIB>2.0.CO;2), 1996.
- Ducrocq, V., Nuissier, O., Ricard, D., Lebeauvin, C. and Thouvenin, T.: A numerical study of three catastrophic precipitating events over southern France. II: Mesoscale triggering and stationarity factors, *Q. J. R. Meteorol. Soc.*, 134, 131–145, doi:[10.1002/qj.199](https://doi.org/10.1002/qj.199), 2008.
- Eden, J. M., Kew, S. F., Bellprat, O., Lenderink, G., Manola, I., Omrani, H. and van Oldenborgh, G. J.: Extreme precipitation
510 in the Netherlands: An event attribution case study, *Weather Clim. Extrem.*, 21, 90–101, doi:[10.1016/j.wace.2018.07.003](https://doi.org/10.1016/j.wace.2018.07.003), 2018.
- Franceinfo: 3 grand est, [online] Available from: <https://france3-regions.francetvinfo.fr/meteo/inondations?r=grand-est>, 2021.
- Funk, T. W.: Forecasting Techniques Utilized by the Forecast Branch of the National Meteorological Center During a Major Convective Rainfall Event, *Weather Forecast.*, 6, 548–564, doi:[24](https://doi.org/10.1175/1520-</p></div><div data-bbox=)



- 515 0434(1991)006<0548:FTUBTF>2.0.CO;2, 1991.
Gaume, E., Bain, V., Bernardara, P., Newinger, O., Barbuc, M., Bateman, A., Blöschl, G., Borga, M., Dumitrescu, A., Daliakopoulos, I., Garcia, J., Irimescu, A., Kohnova, S., Koutroulis, A., Marchi, L., Matreata, S., Medina, V., Preciso, E., Sempere-torres, D., Stancalie, G., Szolgay, J., Tsanis, I., Velasco, D. and Viglione, A.: A compilation of data on European flash floods, *J. Hydrol.*, 367, 70–78, doi:10.1016/j.jhydrol.2008.12.028, 2009.
- 520 George, J. J.: Weather forecasting for aeronautics, Academic Press, New York City. [online] Available from: <https://www.sciencedirect.com/book/9781483233208/weather-forecasting-for-aeronautics>, 1960.
German Weather Service (DWD): Starkregen, Wetter- und Klimalexikon [online] Available from: <https://www.dwd.de/DE/service/lexikon/begriffe/S/Starkregen.html> (Accessed 20 May 2021), 2021.
German Weather Service (DWD) and Gesamtverband der Deutschen Versicherungswirtschaft e. V (GDV): Forschungsprojekt „Starkregen“ - Fachbericht: Eine Zusammenfassung der wichtigsten Ergebnisse des Projekts zum Zusammenhang zwischen Starkregen und versicherten Schäden untersucht von GDV und DWD. [online] Available from: <https://www.gdv.de/resource/blob/63746/ac53789625df198043ea0779329b42d9/fachbericht-data.pdf>, 2019.
Göppert, H.: Auswertung von abgelaufenen Starkregenereignissen über Radarmessungen, *Wasserwirtschaft*, 108(11), 44–50, doi:10.1007/s35147-018-0223-8, 2018.
- 530 Groenemeijer, P. H. and van Delden, A.: Sounding-derived parameters associated with large hail and tornadoes in the Netherlands, *Atmos. Res.*, 83(2-4 SPEC. ISS.), 473–487, doi:10.1016/j.atmosres.2005.08.006, 2007.
Hall, A. J.: Flash flood forecasting, Geneva., 1981.
Hersbach, H., Bell, B., Berrisford, P., Biavati, G., Horányi, A., Muñoz Sabater, J., Nicolas, J., Peubey, C., Radu, R., Rozum, I., Schepers, D., Simmons, A., Soci, C., Dee, D. and Thépaut, J.-N.: ERA5 hourly data on pressure levels from 1979 to present, 535 Copernicus Clim. Chang. Serv. Clim. Data Store, doi:10.24381/cds.bd0915c6, 2018a.
Hersbach, H., Bell, B., Berrisford, P., Biavati, G., Horányi, A., Muñoz Sabater, J., Nicolas, J., Peubey, C., Radu, R., Rozum, I., Schepers, D., Simmons, A., Soci, C., Dee, D. and Thépaut, J.-N.: ERA5 hourly data on single levels from 1979 to present, Copernicus Clim. Chang. Serv. Clim. Data Store, doi:10.24381/cds.adbb2d47, 2018b.
Hersbach, H., Bell, B., Berrisford, P., Hirahara, S., Horányi, A., Muñoz-Sabater, J., Nicolas, J., Peubey, C., Radu, R., Schepers, 540 D., Simmons, A., Soci, C., Abdalla, S., Abellan, X., Balsamo, G., Bechtold, P., Biavati, G., Bidlot, J., Bonavita, M., De Chiara, G., Dahlgren, P., Dee, D., Diamantakis, M., Dragani, R., Flemming, J., Forbes, R., Fuentes, M., Geer, A., Haimberger, L., Healy, S., Hogan, R. J., Hólm, E., Janisková, M., Keeley, S., Laloyaux, P., Lopez, P., Lupu, C., Radnoti, G., de Rosnay, P., Rozum, I., Vamborg, F., Villaume, S. and Thépaut, J. N.: The ERA5 global reanalysis, *Q. J. R. Meteorol. Soc.*, 146(730), 1999–2049, doi:10.1002/qj.3803, 2020.
- 545 Johst, M., Gerlach, N. and Demuth, N.: Starkregen und Hochwasser im Mai/Juni 2018, Mainz, Germany. [online] Available from: http://www.hochwasser-rlp.de/publikationen/bericht_juni_2018.pdf, 2018.
Junker, N. W., Schneider, R. S. and Fauver, S. L.: A study of heavy rainfall events during the great midwest flood of 1993, *Weather Forecast.*, 14(5), 701–712, doi:10.1175/1520-0434(1999)014<0701:ASOHRE>2.0.CO;2, 1999.



- Llasat, M. C., Marcos, R., Llasat-Botija, M., Gilabert, J., Turco, M. and Quintana-Seguí, P.: Flash flood evolution in North-
550 Western Mediterranean, *Atmos. Res.*, 149, 230–243, doi:10.1016/j.atmosres.2014.05.024, 2014.
- Llasat, M. C., Marcos, R., Turco, M., Gilabert, J. and Llasat-Botija, M.: Trends in flash flood events versus convective precipitation in the Mediterranean region: The case of Catalonia, *J. Hydrol.*, 541, 24–37, doi:10.1016/j.jhydrol.2016.05.040, 2016.
- Lupo, A. R.: Atmospheric blocking events: a review, *Ann. N. Y. Acad. Sci.*, doi:10.1111/nyas.14557, 2020.
- 555 Luxemburger Wort: Luxemburger Wort - Archiv, 2021.
- Marchi, L., Borga, M., Preciso, E. and Gaume, E.: Characterisation of selected extreme flash floods in Europe and implications for flood risk management, *J. Hydrol.*, 394(1–2), 118–133, doi:10.1016/j.jhydrol.2010.07.017, 2010.
- Markowski, P. and Richardson, Y.: *Hazards Associated with Deep Moist Convection*, edited by L. John Wiley & Sons., 2010.
- Mathias, L.: Major flood event in the Mullerthal region on 1 June 2018: event analysis and predictability, *MeteoLux*, (June
560 2018), 1–17, 2019.
- Mathias, L.: Synoptic-mesoscale analysis of the flash-flood-producing thunderstorm over the Vallée de l’Ernz on 22 July 2016, *MeteoLux*, (July 2016), 1–18, 2021.
- Meischner, P.: *Weather Radar: Principles and Advanced Applications*, Springer Berlin Heidelberg, Berlin., 2014.
- Mohr, S., Wilhelm, J., Wandel, J., Kunz, M., Portmann, R., Punge, H. J., Schmidberger, M., Quinting, J. F. and Grams, C. M.:
565 The role of large-scale dynamics in an exceptional sequence of severe thunderstorms in Europe May–June 2018, *Weather Clim. Dyn.*, 1(2), 325–348, doi:10.5194/wcd-1-325-2020, 2020.
- Müller, E. N. and Pfister, A.: Increasing occurrence of high-intensity rainstorm events relevant for the generation of soil erosion in a temperate lowland region in Central Europe, *J. Hydrol.*, 411(3–4), 266–278, doi:10.1016/j.jhydrol.2011.10.005, 2011.
- Muñoz Sabater, J.: ERA5-Land hourly data from 1981 to present, Copernicus Clim. Chang. Serv. Clim. Data Store,
570 doi:10.24381/cds.e2161bac, 2019.
- Nuissier, O., Ducrocq, V., Ricard, D., Lebeaupin, C. and Anquetin, S.: A numerical study of three catastrophic precipitating events over southern France. I: Numerical framework and synoptic ingredients, *Q. J. R. Meteorol. Soc.*, 134, 111–130, doi:10.1002/qj, 2008.
- Owen, P. W., Roberts, G., Prigent, O., Markus, R., Tanguy, B., Bridgford, M., Katharina, B., Ciabatti, I., Gatter, L., Gilson,
575 V., Kubat, J., Laanes, L., Simeonova, R., Critoph, H. and Annette, Z.: Flood Directive: progress in assessing risks, while planning and implementation need to improve, Luxembourg., 2018.
- Pfister, L., Kwadijk, J., Musy, A., Bronstert, A. and Hoffmann, L.: Climate change, land use change and runoff prediction in the Rhine-Meuse basins, *River Res. Appl.*, 20(3), 229–241, doi:10.1002/rra.775, 2004.
- Pfister, L., Faber, O., Hostache, R., Iffly, J. F., Matgen, P., Minette, F., Trebs, I., Bastian, C., Göhlhausen, D., Meisch, C. and
580 Patz, N.: Crue éclair du 22 juillet 2016 dans la region de Larochette - Étude mécanistique et fréquentielle réalisée en 2018 pour le compte de l’Administration de la gestion de l’eau, Esch-sur-Alzette. [online] Available from: <https://eau.gouvernement.lu/dam-assets/publications/crue-éclair-du-22-juillet-2016/1812-LIST-BrochureCrueEclair.pdf>,



- 2018.
- Pfister, L., Douinot, A., Hostache, R., François, I. J., Matgen, P., Minette, F., Bastian, C., Gilbertz, C., Göhlhausen, D., Meisch,
585 C. and Patz, N.: Crues subites 2018 - Étude mécanistique et fréquentielle des crues subites de 2018 au Luxembourg, Esch-
sur-Alzette. [online] Available from: [https://eau.gouvernement.lu/fr/services-aux-](https://eau.gouvernement.lu/fr/services-aux-citoyens/publications/2021/brochures/Cruces-subites-2018.html)
[citoyens/publications/2021/brochures/Cruces-subites-2018.html](https://eau.gouvernement.lu/fr/services-aux-citoyens/publications/2021/brochures/Cruces-subites-2018.html), 2020.
- Piper, D., Kunz, M., Ehmele, F., Mohr, S., Mühr, B., Kron, A. and Daniell, J.: Exceptional sequence of severe thunderstorms
and related flash floods in May and June 2016 in Germany – Part 1: Meteorological background, *Nat. Hazards Earth Syst. Sci.*,
590 16, 2835–2850, doi:10.5194/nhess-16-2835-2016, 2016.
- Pučík, T., Groenemeijer, P., Rýva, D. and Kolář, M.: Proximity soundings of severe and nonsevere thunderstorms in central
Europe, *Mon. Weather Rev.*, 143(12), 4805–4821, doi:10.1175/MWR-D-15-0104.1, 2015.
- Pučík, T., Groenemeijer, P., Rädler, A. T., Tijssen, L., Nikulin, G., Prein, A. F., Meijgaard, E. van, Fealy, R., Jacob, D. and
Teichmann, C.: Future changes in European severe convection environments in a regional climate model ensemble, *J. Clim.*,
595 30(17), 6771–6794, doi:10.1175/JCLI-D-16-0777.1, 2017.
- Rädler, A. T., Groenemeijer, P., Faust, E. and Sausen, R.: Detecting severe weather trends using an additive regressive
convective hazard model (AR-CHaMo), *J. Appl. Meteorol. Climatol.*, 57(3), 569–587, doi:10.1175/JAMC-D-17-0132.1, 2018.
- Rauber, R. M., Charlevoix, D. J. and Walsh, J. E.: Severe and hazardous weather: an introduction to high impact meteorology,
3rd ed., Kendall/Hunt Publishing Company, Dubuque, Iowa., 2008.
- 600 Ruiz-Villanueva, V., Borga, M., Zoccatelli, D., Marchi, L., Gaume, E. and Ehret, U.: Extreme flood response to short-duration
convective rainfall in South-West Germany, *Hydrol. Earth Syst. Sci.*, 16(5), 1543–1559, doi:10.5194/hess-16-1543-2012,
2012.
- Séchet, G.: *Météo extrême - au coeur des phénomènes climatiques spectaculaires*, Hugo Image, Paris., 2019.
- Sikorska-Senoner, A. E. and Seibert, J.: Flood-type trend analysis for alpine catchments, *Hydrol. Sci. J.*, 65(8), 1281–1299,
605 doi:10.1080/02626667.2020.1749761, 2020.
- Strangeways, I.: *Precipitation : theory, measurement and distribution*, Cambridge University Press, Cambridge., 2007.
- Taszarek, M., Brooks, H. E. and Czernecki, B.: Sounding-derived parameters associated with convective hazards in Europe,
Mon. Weather Rev., 145(4), 1511–1528, doi:10.1175/MWR-D-16-0384.1, 2017.
- Taszarek, M., Allen, J. T., Brooks, H. E., Pilguy, N. and Czernecki, B.: Differing trends in United States and European Severe
610 Thunderstorm Environments in a Warming Climate, *Bull. Am. Meteorol. Soc.*, 102(2), E296–E322,
doi:<https://doi.org/10.1175/BAMS-D-20-0004.1>, 2021a.
- Taszarek, M., Allen, J. T., Marchio, M. and Brooks, H. E.: Global climatology and trends in convective environments from
ERA5 and rawinsonde data, *Clim. Atmos. Sci.*, 4(1), 1–11, doi:10.1038/s41612-021-00190-x, 2021b.
- Vogel, K., Ozturk, U., Riemer, A., Laudan, J., Sieg, T., Wendi, D. and Agarwal, A.: Die Sturzflut von Braunsbach am 29 .
615 Mai 2016 – Entstehung , Ablauf und Schäden eines „ Jahrhundertereignisses “. Teil 2 : Geomorphologische Prozesse und
Schadensanalyse, *Hydrol. und Wasserbewirtschaftung*, 61(3), 163–175, doi:10.5675/HyWa, 2017.



- Weigl, E. and Winterrath, T.: Radargestützte Niederschlagsanalyse und -vorhersage (RADOLAN, RADVOR-OP), *Promet*, 35(1–3), 76–86, 2009.
- 620 Weigl, E., Reich, T., Lang, P., Wagner, A., Kohler, O., Gerlach, N. and Bartels, H.: Routineverfahren zur Online-Aneicherung der Radarniederschlagsdaten mithilfe von automatischen Bodenniederschlagsstationen (Ombrometer), German Weather Service: Hydrometeorology department, Offenbach am Main., 2004.
- Westermayer, A. T., Groenemeijer, P., Pistotnik, G., Sausen, R. and Faust, E.: Identification of favorable environments for thunderstorms in reanalysis data, *Meteorol. Zeitschrift*, 26(1), 59–70, doi:10.1127/metz/2016/0754, 2017.
- 625 Winterrath, T., Brendel, C., Hafer, M., Junghänel, T., Klameth, A., Walawender, E., Weigl, E. and Becker, A.: Erstellung einer radargestützten Niederschlagsklimatologie, Reports of the German Weather Service, No. 251, Offenbach am Main., 2017.
- WMO: Flash Flood Guidance System (FFGS) with Global Coverage, World Meteorol. Organ. [online] Available from: <https://public.wmo.int/en/projects/ffgs> (Accessed 16 December 2021), 2017.